**Hydrology and
Earth System
Sciences
Discussions**

A multi-scale "soil water structure" model based on the pedostructure concept

E. Braudeau[1,3]**, R. H. Mohtar**[2]**, N. El Ghezal**[3]**, M. Crayol**[4]**, M. Salahat**[5]**, and
P. Martin**[6]

[1]BIOEMCO, IRD, Centre de Recherche Ile de France, 93143, Bondy, France
[2]Agricultural and Biological Engineering, Purdue University, West Lafayette, Indiana, USA
[3]IRD, Pôle de Recherche Agroenvironnementale de la Martinique (PRAM), Martinique
[4]CIRAD, Pôle de Recherche Agroenvironnementale de la Martinique(PRAM), Martinique
[5]Natural Resources and Environment Department, the Hashemite University, Zarka, Jordan
[6]CIRAD, TA 70/PS III, 34398 Montpellier cedex 5, France

Correspondence to: E. Braudeau (erik.braudeau@ird.fr)

Abstract

Current soil water models do not take into account the internal organization of the soil medium and, a fortiori, the physical interaction between the water film surrounding the solid particles of the soil structure, and the surface charges of this structure. In that sense they empirically deal with the physical soil properties that are all generated from this soil water-structure interaction. As a result, the thermodynamic state of the soil water medium, which constitutes the local physical conditions, namely the pedo-climate, for biological and geo-chemical processes in soil, is not defined in these models. The omission of soil structure from soil characterization and modeling does not allow for coupling disciplinary models for these processes with soil water models. This article presents a soil water structure model, Kamel®, which was developed based on a new paradigm in soil physics where the hierarchical soil structure is taken into account allowing for defining its thermodynamic properties. After a review of soil physics principles which forms the basis of the paradigm, we describe the basic relationships and functionality of the model. Kamel® runs with a set of 15 soil input parameters, the pedo-hydral parameters, which are parameters of the physically-based equations of four soil characteristic curves that can be measured in the laboratory. For cases where some of these parameters are not available, we show how to estimate these parameters from commonly available soil information using published pedotransfer functions. A published field experimental study on the dynamics of the soil moisture profile following a pounded infiltration rainfall event was used as an example to demonstrate soil characterization and Kamel® simulations. The simulated soil moisture profile for a period of 60 days showed very good agreement with experimental field data. Simulations using input data calculated from soil texture and pedotransfer functions were also generated and compared to simulations of the more ideal characterization. The later comparison illustrates how Kamel® can be used and adapt to any case of soil data availability. As physically based model on soil structure, it may be used as a standard reference to evaluate other soil-water models and also pedotransfer functions at a given location or

agronomical situation.

1 Introduction

Representing the top soil structured medium with special attention to its hierarchy of scales is important to the modeling and understanding of the dynamics of water flow
5 and water storage in soil for agronomic needs and for the fate of pollution at the field, farm and watershed scales. The later is critically relevant from an agronomic standpoint since agriculture continues to be the main source of pollution. Single pore representation of the soil water medium is very common in agronomic models such as GRASIM (Mohtar et al., 1997) or CROPSYST (Stöckle et al., 2003). The tendency for modeling
10 water flow and solute transport in structured soil is to distinguish two domains, micro- and macropore, in an implicit soil horizon REV (Representative Elementary Volume) (Othmer et al., 1991; Chen et al., 1993; Gerke and Van Genuchten, 1993; Katterer et al., 2001; Logsdon, 2002; Simunek et al., 2001, 2003). Only few of these models consider the soil medium as a structured medium with aggregates and none used the
15 notion of primary peds, which represent the first level of organization of the primary particles into aggregates (Brewer, 1964). Consequently, the swelling-shrinkage properties of these primary peds within the soil structure (Braudeau and Bruand, 1993) and the resulting hydro-structural properties of the soil medium (Braudeau et al., 2004, 2005) is not physically modeled.

20 Additionally, as long as these characteristics of the soil organization and structure are not defined nor integrated in soil-water models, the modeling of biophysical and chemical processes in the soil medium cannot be physically linked to this soil organization and structure, thus, cannot be physically related to any type of soil characterized by its hydro-structural functioning.

25 Braudeau et al. (2004) presented a new conceptual and functional model of the internal soil organization where the soil horizon is made up of non rigid primary peds arranged in that which was called pedostructure. This representation led Braudeau

1113

and Mohtar (2009) to define a new paradigm for modeling soil water that takes into account the hierarchical internal organization of the soil medium, and thus allowing for: i) defining the local thermodynamic state of this medium at a point of soil in depth and ii) transferring the information data through the different functional scales, from the pedostructure, to the soil horizon, the pedon and the soil mapping unit. A computer model simulating the hydro-structural functioning of the pedon, named Kamel®, was developed based on this paradigm (Braudeau, 2006). A short outline is given in Appendix D.

The objectives of the paper are to i) describe the basic principles of Kamel® along with its state variables, parameters and equations used; ii) present a procedure for estimating the model input parameters using pedotransfer functions and iii) demonstrate how the model can be used to simulate a soil water movement in the field using an example from literature including how to estimate soil parameters from measured soil data given in the example.

2 Basic principles of the soil water structure model Kamel®

2.1 The Structural Representative Elementary Volume (SREV)

In order to take into account the soil structure in the well-known notion of Representative Elementary Volume (REV) in soil physics (Bear, 1972), Braudeau and Mohtar (2009) introduced the notion of "Structural Representative Elementary Volume" (SREV). According to the qualitative definition of a REV, the SREV is the smallest volume representative of the soil medium where the pedohydral properties are the same everywhere in the medium at the scale of the structural unit of soil that is considered (clod, horizon, pedon etc.). However, unlike the REV, the SREV is virtually delimited by an enclosure which is permeable to air, water, or salts fluxes but not to solids that compose the structure. This description defines any SREV as a volume V comprising a fixed mass of solids belonging to the structure, m_S, such that its specific volume,

defined as $\overline{V}=V/m_S$, depends only on the changes in the content of its mobile phases, water and air, since $dm_S=0$ in every case. This allowed writing the specific thermodynamic potential of a SREV of the soil medium in reference to the structural mass (m_S) enclosed in the delimitation such that:

$$d\overline{G} = -\overline{S}dT + \overline{V}dP + \mu_w dW - \overline{A}d\mu_a \qquad (1)$$

where $\overline{G}=G/m_S$; $\overline{S}=S/m_S$; $\overline{V}=V/m_S$; $W=m_W/m_S$ and $\overline{A}=m_a/m_S$, respectively, the specific Gibbs energy, specific entropy, specific structural volume, specific water content and specific air content. The controlled variables of state are T, P, W, and μ_a, respectively the temperature, the pressure exerted on the SREV, water content and air potential. Equation (1) characterizes the variation of the specific thermodynamic potential of a SREV of soil with a change of T, P, W, and air pressure in the medium.

This description gives SREVs the following properties:

1. The soil medium SREV is physically characterized by extensive specific state variables like $\overline{G}, \overline{S}, \overline{V}, \overline{A}$ and W (extensive variables of the soil medium SREV divided by the structural mass of the SREV), in addition to the classical intensive variables such as temperature T, pressure P and soil water potential μ_w.

2. The *homogeneity* of a soil medium can be defined as a uniform distribution of the functions of state $\overline{S}$, $\overline{V}$, $\overline{A}$ and μ_w, in regard to the state variables T, P, W and μ_a. Practically, neglecting the role of $\overline{S}$ and knowing that $\overline{A}=\overline{V}-W-\overline{V}_S$ ($\overline{V}_S$ being the specific volume of the solid phase), a soil horizon will be considered structurally homogeneous against water if the shrinkage curve, $\overline{V}(W)$, and the water potential curve, $\mu_w(W)$, are the same for a given P and T, everywhere in the medium of the horizon.

3. Specific extensive variables of an SREV can be nested with respect to the hierarchical organization of the medium. This property allowed defining the descriptive variables of the soil medium at its various functional levels organization, namely

1115

the pedon, horizon, pedostructure, primary peds and primary particles (Table 1, Braudeau and Mohtar, 2009). The representation and discretization of the pedon needed for modeling and that result from these concepts are summarized hereafter.

2.2 Pedon representation and modeling

2.2.1 Primary peds and pedostructure

Brewer (1964) introduced the following concepts of primary ped and S-matrix: "A ped is an individual natural soil aggregate consisting of a cluster of primary particles and separated from adjoining peds by surfaces of weakness which are recognizable as natural voids or by occurrence of cutans."

"Primary peds are thus the simplest peds occurring in a soil material. They cannot be divided into smaller peds, but they may be packed together to form compound peds of higher level of organization. The S-matrix of a soil material is the material within the simplest (primary) peds, or composing apedal soil materials, in which the pedological features occur; it consists of plasma, skeleton grains, and voids that do not occur in pedological features other than plasma separations."

Braudeau et al. (2004) complete this morphological definition of primary peds with a functional definition based on the determination of air entry point in the plasma using the continuously measured shrinkage curve (Braudeau and Bruand, 1993). They introduced the term of pedostructure which is the assembly of primary peds and characterizes the structure of a soil horizon (Fig. 1). These definitions allowed the physical characterization of the primary peds properties, inside the pedostructure, using the shrinkage curve continuously measured on a soil sample in the laboratory. They allowed also separating the primary peds of a soil sample in laboratory using the soil fractionation method of Colleuille and Braudeau (1996).

Therefore, variables and parameters are defined for both distinct media owing to the pedostructure: inside and outside of the primary peds: $\overline{V}_{mi}$, Vp_{mi}, W_{mi}, h_{mi}, k_{mi},

Vp_{ma}, W_{ma}, h_{ma}, k_{ma} (see the nomenclature and definition in Table 1) subscripts mi and ma referring to as micro (intra primary peds) and macro (inter primary peds).

Braudeau and Mohtar (2009) showed that the pedostructure corresponds to the SREV of the soil horizon medium as assembly of primary peds and primary particles in about 100 cm^3 of soil sample. All organization variables are relative to the same mass of solids contained in the SREV and relationships between them express the structure hierarchy such as:

$$\overline{V} = \overline{V}_{mi} + Vp_{ma} \text{ and } \overline{V}_{mi} = Vp_{mi} + \overline{V}_S$$

where $\overline{V}_S$ is the specific volume of pedostructure primary particles.

2.2.2 Discretization of the Pedon according to the SREV concept

Modeling water and gas transfer through the pedon requires discretization of the medium into representative elementary layers at the scale of the pedon. To keep all properties of the pedostructure at the scale of the layer, the latter must be defined according to the SREV concept as Structure Representative Elementary Layer (SREL) (Braudeau and Mohtar, 2009) which consists of the lateral extension of the horizon SREV over the width of the pedon (Fig. 1). In general, fine layers of near 0.2 dm thickness can be taken as SRELs at the pedon scale. The pedon must be wide enough so it can be representative of the soil in regards of the size of pedologic features like fissures, stones or other that may be observed at this scale level.

Thus, descriptive variables of a SREL include those of the pedostructure plus few new features (roots, biogenic macropores, stones . . .) of which volumes are related to the total mass of the layer. However, the mass of pedostructure included in the SREL is more convenient to be taken as reference rather than the total mass of the layer. This allows for not changing the variables and properties of the pedostructure as part of the new SREL set of variables. As an example, suppose that a sample, large enough to represent the horizon, has a dry mass M and comprises two kinds of

1117

pedostructure of specific volumes: $\overline{V_1}$ and $\overline{V_2}$ and masses: m_1 and m_2; and stones of specific volumes: $\overline{V}_{\text{stones}}$ and mass m_{stone}, such that $M = m_1 + m_2 + m_{\text{stone}}$. The specific volume of the SREL should be written such as:

$$\overline{V}_{\text{layer}} = \overline{V}_1 \frac{m_1}{m_1 + m_2} + \overline{V}_2 \frac{m_2}{m_1 + m_2} + \overline{V}_{\text{stone}} \frac{m_{\text{stone}}}{m_1 + m_2} + \frac{V_{\text{fiss}}}{m_1 + m_2} + \frac{V_{\text{bio}}}{m_1 + m_2} \qquad (2)$$

5   where $\overline{V}_{\text{bio}}$ is the pore volume created by the biological activity (roots, fauna . . .) related to the total pedostructure mass; $\overline{V}_{\text{fiss}}$ the volume of fissures and cracks appearing as the horizon dries.

According to the SREV definition, the reference mass of solids in a layer is associated with its delimitation. Thus, the discretization of the pedon in layers (Fig. 1) must be
10   conducted in such a manner that the reference mass of solids in the layer can be calculated. Since SREV position in depth (z) and thickness are controlled by the specific volume of the layer ($\overline{V}_{\text{layer}}$), horizons in the pedon must be considered, for discretization, at uniform water content and near saturation in order to avoid opened fissures due to shrinkage.

15   We note that the spatial distribution of variables in the SREL is not defined and not known. However, while the intensive variables, like h_{mi} and h_{ma}, can be considered as averaged values in the SREL, its specific extensive variables like W, W_{ma} or W_{mi}, etc. correspond to total contents of components in the layer. This is important to consider in modeling water transfer using finite elements calculation. In fact, discretization of the
20   pedon into SRELs allows modeling internal processes that could not be modeled before using the classical REV concept; for example, the opening of the vertical porosity ($\overline{V}_{\text{fiss}}$) when a wetted soil is drying and the conjoint dynamics of the water and the layer in the pedon, which are developed below.

2.2.3 Modeling vertical fissures and cracks

Position and thickness of the layers are governed by $\overline{V}_{\text{layer}}$ which is known in terms of W according to the pedostructure shrinkage curve equation. Because of the difference between the one-dimensional volume change of the soil layer as a function of water content and the three-dimensional volume change of the pedostructure, the relationship between the two SREVs (soil layer and pedostructure) is, in case of an isotropic shrinkage of the pedostructure (Braudeau et al., 2004b):

$$\overline{V}_{\text{layer}} = \left(\overline{V} + 2\overline{V}_D\right)/3 \quad \text{and} \quad Vp_{\text{fiss}} = \overline{V}_{\text{layer}} - \overline{V} = 2\left(\overline{V}_D - \overline{V}\right)/3 \tag{3}$$

V_D being the specific volume of the pedostructure at water content W_D corresponding to the beginning of shrinkage of the primary peds, such that:

$$\overline{V}_{\text{layer}} = \overline{V} \quad \text{for} \quad W > W_D. \tag{4}$$

2.3 Thermodynamic functions of the pedostructure

The soil shrinkage curve and the soil water potential curve are two of the four thermodynamic state functions of the structured soil medium relative to changes in water content. These functions depend on the internal organization of the soil medium and reveal the interaction between soil water and the surface of solids composing the pedostructure (primary peds and their assembly). In order to determine their physical equations, new variables describing the soil organization were defined (Braudeau et al., 2004a). A brief summary of this organization and structure is described in this section.

2.3.1 Pores systems and types of water pools

For interpreting the shrinkage curve (SC) Braudeau et al. (2004a) define two pools of water in the two pore systems (Fig. 2) corresponding to inside and outside primary

peds: swelling water, and non-swelling water. Swelling water occupies a pore space acquired by the spacing of particles or aggregates under the effect of osmotic pressure. Its removal from the sample causes shrinkage of the concerned pore system. Non swelling water, on the other hand, occupies an interstitial pore space and is replaced by air (or water vapor) when it leaves the pore system; its loss causes little or no shrinkage. During drying, each linear phase of the shrinkage curve is caused by the predominant departure of one type of water from either the micro- or the macro-pore system. Braudeau et al. (2004) defined four water pools that contribute to water flow upon drying successively from a soil sample initially at saturation: they were called in reference to the corresponding shrinkage phase, interpedal, structural, basic and residual: w_{ip}, w_{st}, w_{bs}, w_{re}.

Equations of these water pools contents at the state of equilibrium represented by the shrinkage curve and their characteristic parameters are presented in Appendix A.

According the definition of the water pools, the variation of the pedostructure specific volume is written such as:

$$d\overline{V} = K_{bs}dw_{bs} + K_{ip}dw_{ip} \tag{5}$$

where K_{bs} is the slope of the basic linear shrinkage phase and K_{ip}=1 dm^3/kg is the slope of the asymptote to the curve at saturation, parallel to the saturation line and represents the interpedal shrinkage at saturated state (Fig. 3). They represent the pedostructure volume change caused by the change in content of the *swelling water pools w_{bs} and w_{ip}*. The slopes K_{bs} and K_{ip} are considered as structural parameters of the pedostructure, linking the macroscopic assembly level to the water pools levels. As an example:

$$K_{bs} = \partial\overline{V}/\partial w_{bs} = \partial\overline{V}/\partial\overline{V}_{mi} \tag{6}$$

where $\overline{V}_{mi}$ is the specific volume of primary peds (Table 1).

Figure 3 shows different encountered shapes of shrinkage curve, depending on the texture, type of clay and on the aggregated structure of the soil medium. Each graph

of the figure represents a continuously measured curve of a soil sample, the fitted curve (Eq. 5) and a curve corresponding to the same material (same parameters for the primary peds) but with a change of structural properties (porosity and cohesion of the assembly) represented by a change in bulk density and parameters of w_{ip}: k_L and W_L (Table 2). This difference in shape depending on the structural stability is important for loamy or silty soils of which $K_{bs} \ll 1$ (Shaffer et al., 2007). One can appreciate on Fig. 3 the great difference that may exist between W_L and W_{sat}, depending on the type of shrinkage curve. W_L is at the intersection of the basic shrinkage curve $\overline{V}_{mi}(W)$ and the saturated line while W_{sat} is at the junction of the shrinkage curve $\overline{V}(W)$ and the saturated line. This point is not stable and is better defined and determined as the soil water content corresponding to a soil water suction $h=0$ kPa.

2.3.2 Inter and intra primary peds water potentials: the thermodynamic approach

The usual approach for modeling soil water potential emphasizes the geometrical aspect of soil structure, restricting the soil water potential to the interfacial tension of the air-water meniscus. Its curvature determines the potential according to the Laplace-Kelvin law and it is assimilated to the pore radius r_c for which all pore segments with sides shorter than $2r_c$ are filled with water. This approach does not make any reference to swelling pressure, caused by osmotic or hydration force or interaction between solid surfaces and water.

Braudeau and Mohtar (2004) showed that the thermodynamical approach of Low (1987), Voronin (1980) and Berezin (1983) calls for other notions than the interfacial meniscus curvature. According to Low (1987), water is arranged in layers at the surface of the particles and a swelling pressure is observed depending on the thickness of the water film (τ) and the specific surface area of the soil particles. In this approach, the thickness t of the film of water at the surface of the unsaturated pores is used as the variable. The difference with the Laplace-Kelvin approach is that the change of water is simply related to τ by $dW = S d\tau$ where S is the specific surface area of the solids.

The swelling pressure is analogous to an osmotic pressure but, as explained by Low (1987), is primarily due to the interaction of water molecules with the surface of the clay particles which modifies the structure of the surrounding water layers.

According to this approach, the water suction pressure intra and extra primary peds, h_{mi} and h_{ma} (kPa) are expressed in terms of W_{mi} and W_{ma} such as:

$$h_{ma} = Ps_{ma} - Ps_{ma}^o = \rho_w E_{ma}\left(1/\left(W_{ma} + \sigma\right) - 1/\left(W_{sat} - W_M + \sigma\right)\right) \tag{7}$$

$$h_{mi} = Ps_{mi} - Ps_{mi}^o = \rho_w E_{mi}\left(1/\left(W_{mi} - W_N\right) - 1/\left(W_M - W_N\right)\right) \tag{8}$$

where ρ_w is the water bulk density (1 kg/dm^3); Ps_{mi} and Ps_{ma} (kPa) are the swelling pressure inside and outside the primary peds, E_{mi} and E_{ma} are the potential energies of the solid phase resulting from the external surface charge of clay particles, inside and outside the primary peds, in joules/kg of solids; σ (kg water/kg soil) is a part of the micropore water at interface with interpedal water. Both terms Ps_{mi^o} and Ps_{ma^o} represent the swelling pressure at saturation, inside and outside of the primary peds, respectively, namely when $W_{ma}=W_{maSat}=W_{sat}-W_M$; and $W_{mi}=\max(W_{mi})=W_M$, where W_M and W_N are two parameters of the water pools equilibrium equations given in Appendix A.

2.4 Dynamics of water within and through the soil layer

2.4.1 Dynamic of water through the interped space

Braudeau and Mohtar (2009) distinguished three types of transport represented in Fig. 4 that schematizes the functional compartments of a pedostructure unit and its hydraulic functioning: (1) a local transport within the pedostructure (SREV of the horizon) corresponding to a water exchange between the both pore spaces inside and outside primary peds; (2) a transport through the pedostructure that involves only the interped water, W_{ma}; and (3) a flux across cells that is accounted for between neighboring micro pores due to differences in micro potential.

We can assume then that the water transfer micro-micro and micro-macro have intrinsically the same transfer rate coefficient k_{mi} (kg$_{\text{microwater}}$ kg$_{\text{soil}}^{-1}$ kPa^{-1} s^{-1}) defined by Braudeau and Mohtar (2006) but that in the case of the micro-micro transfer this coefficient will depend on the contact area between primary peds. Accordingly, neglecting the lateral water transfer, equations of transfer for W_{ma} and W_{mi} are written such as:

$$\frac{dW_{ma}}{dt} = \rho_w \overline{V} \frac{\partial}{\partial z} \left(k_{ma} \left(-\frac{dh_{ma}}{dz} + 1 \right) \right) - k_{mi} (h_{mi} - h_{ma}) \tag{9}$$

where z is the deep (positive upward); and

$$\frac{dW_{mi}}{dt} = k'_{mi} \Delta_z h_{mi} + k_{mi} (h_{mi} - h_{ma}) \tag{10}$$

where $\Delta_z h_{mi}$ is the difference of suction pressure between the pedostructure unit and the adjacent units. In these equations, suctions h_{ma} and h_{mi} are expressed in dm of height of water (equivalent to kPa), z in dm and k_{ma} in dm/s.

However, considering that contact areas (s) between primary peds are small in regard to their external surfaces (S), $k'_{mi} = (s/S) k_{mi}$ can be neglected in Eq. (10) and the transfer of water from micro to micro is only possible through the macro water. In fact, the transfer of water between two layers (or pedostructure units) will concern W_{ma} only (Eq. 9) leading to consider W_{ma} as exactly the mobile water and W_{mi}, the (temporary) immobile water.

2.4.2 Soil hydraulic conductivity

The hydraulic conductivity k_{ma} in Eq. (9) is considered with respect to the macropore water content, W_{ma}, which comprises the interped water of the pedostructure plus eventually the water present in the biogenic pores of the SREL defined in Eq. (2). Since the micro-micro water flux between layers is neglected compared to the macro-macro and micro-macro water fluxes, $k_{ma}(W_{ma})$ is equal to the classical hydraulic conductivity k, which is described in literature by several empirical equations in terms of the total water content, W, or the water suction pressure, h.

Based on considerations presented in the Appendix B it is assumed that the hydraulic conductivity k_{ma} is described by two exponential functions of W_{ma} which are different at high (near saturation) as compared to low water content (near W_C). The two exponential equations are written such as:

$$k_{ma} = k_{maM}\exp(\alpha_M W_{ma}) \text{ and } k_{ma} = k_{ma^o}\exp(\alpha_o W_{ma}) \tag{11}$$

for the high and low ranges of W_{ma}, respectively defined on the shrinkage curve: high and low ranges of W_{ma} corresponding to (W_{sat} to W_M) and (W_M to W_C), respectively. The two sets of parameters (k_{maM}, α_M and k_{ma^o}, α_o) are characteristics of these two ranges of water content.

In order to have only one equation for describing the hydraulic conductivity curve but keeping the distinction between the two ranges of conductivities, Eq. (11) were combined in a logistic such that:

$$k_{ma} = \frac{k_{maM}\exp(\alpha_o W_{ma})}{k_{maM}/k_{ma^o} + \exp((\alpha_o - \alpha_M)W_{ma})} \tag{12}$$

This equation represents the conductivity curve for Kamel® model and has four parameters: k_{maM}, α_M, k_{ma^o}, and α_o. The first two parameters can be measured in situ using an infiltrometer (Angulo-Jaramillo et al., 2000) or on non-disturbed samples in laboratory using the method presented in Bruckler et al. (2002); the last two parameters relative to low macro water content (near point C of the shrinkage curve) can be measured by the evaporation method (Wendroth et al., 1993a).

2.4.3 Dynamic of water within the pedostructure

The two opposite dynamics of the pedostructure, swelling and shrinking, are supposed to be governed by the same conceptual process that is the water exchange between the primary peds and the interped pore space. Braudeau and Mohtar (2006) validated in a particular case (aggregates immersed in water) the following equation where the

water exchange between the two media is proportional to the difference in their suction pressure:

$$\frac{dW_{mi}}{dt} = k_{mi}\,(h_{mi} - h_{ma}) \tag{13}$$

In this equation, k_{mi} is the transfer rate coefficient ($\text{kg}_{\text{microwater}}\,\text{kg}_{\text{soil}}^{-1}\,\text{kPa}^{-1}\,\text{s}^{-1}$) for the absorption-desorption of the interped water by the primary peds. This coefficient expresses the velocity of the last layer of water on the surface of the clay particles entering or leaving the primary peds. We assume that this transfer rate coefficient k_{mi} is constant in the range of water content [W_B–W_{sat}] and that Eq. (13) can be generalized to the shrinkage ($dw_{bs}/dt<0$) as well as the swelling ($dw_{bs}/dt>0$). Braudeau and Mohtar (2006) showed that the micro-macro water exchange coefficient, k_{mi}, can be calculated by:

$$k_{mi} = \frac{(W_M - W_N)^2}{\rho_w E_{mi}}\frac{0.1931}{t_{1/2}} \tag{14}$$

where $t_{1/2}$ is the time of half swelling in seconds at $w_{bs}=\max(w_{bs})/2=(W_M - W_N)/2$. This time to half swelling is a characteristic of the kind of plasma in the soil (in fact the primary peds constitution) and is easily determined in laboratory using the measurement of the swelling of aggregates immersed in water versus time. The literature lacks descriptions about measurements of the water absorption by aggregates versus time or soil swelling versus time, limited mentions of this phenomenon can be found in Quirk and Panabokke (1962) and McIntyre et al. (1982). However, these were not interpreted in terms of swelling of primary peds impacting the soil structure. The time of half charge can be graphically estimated from the time dependent swelling curves such as those measured by Braudeau and Mohtar (2006); therefore, we retained $t_{1/2}$ as input parameter for Kamel® rather than k_{mi}.

2.5 Computation of water fluxes

The discretization of the soil horizons into soil layers and the nomenclature used are shown in Fig. 5, where the fluxes $F1$ and $F2$ are represented for each layer at every time step along with the thickness H_i, the water suction h_i (h_{ma}) and the conductivity k_i (k_{ma}) of the layer.

Each layer is small enough (2 cm thick is recommended) such that the state variables keep the same values everywhere in the layer and the resulting conductivity of the portion delimited by two dashed lines ($k_{i-1/2}$ or $k_{i+1/2}$) can be approximated by the arithmetic average of the two corresponding conductivities:

$$k_{i-1/2} = (k_{i-1} + k_i)/2 \text{ and } k_{i+1/2} = (k_i + k_{i+1})/2. \tag{15}$$

At each time step, for the layer i, fluxes through the upper and lower surfaces of the soil layer i, F1$_i$ and F2$_i$, are calculated:

$$\text{F1}_i = \frac{k_{i-1} + k_i}{H_{i-1} + H_i} \left(h_{i-1} - h_i - \frac{H_{i-1} + H_i}{2} \right) \tag{16}$$

and

$$\text{F2}_i = \frac{k_i + k_{i+1}}{H_i + H_{i+1}} \left(h_i - h_{i+1} - \frac{H_i + H_{i+1}}{2} \right) \tag{17}$$

The conditions are such that F2$_{i-1}$=F1$_i$ and F2$_i$=F1$_{i+1}$, and that F2 and F1 cannot be greater than the available space in the receiving layer nor can they extract more water than possible from the providing layer. At the inferior limit of the profile (i=end), F2$_{\text{end}}$ is calculated as if the layer outside has the same characteristics as the last layer of the profile but with k and h being taken as k_{end} and h_{end} calculated at the previous time step $t-1$.

Under these conditions, changes in W_i due to F_1 and F_2 for each step is then calculated by

$$\Delta W_i = \rho_w \overline{V}_{\text{layer}_i} (\text{F2}_i - \text{F1}_i)/H_i \tag{18}$$

The change ΔW is initially considered as a change in W_{ma}, which provokes temporarily a change in h_{ma} and then an imbalance between W_{mi} and W_{ma}. This is corrected when new values of W_{mi} and W_{ma} are computed. The transfer of water between the two pore systems during the time step is calculated as:

$$\Delta W_{mi} = -\Delta W_{ma} = k_{mi} (h_{mi} - h_{ma}) \tag{19}$$

3 Materials and Methods

3.1 Experimental field data used

We applied Kamel$^{®}$ model for simulating a field drainage experiment reported by Davidson et al. (1969) starting from two sets of parameters: i) pedohydral parameters calculated from the soil characteristics given by these authors, namely, the tensiometric and conductivity curves, and the bulk density at every 30 cm depth; and ii) pedohydral parameters calculated from soil characteristics estimated according to the pedotransfer functions (PTFs) gathered by Saxton and Rawls (2006). Davidson et al. (1969) measured field water redistribution and drainage during 60 days following saturation of the soil profile. The soil characteristics given in the article for each depth (30 cm interval) are 1) the water potential curve in the range 0 to 50 kPa, which was measured in the laboratory on soil core samples; 2) the bulk density; and 3) the two parameters of the exponential form of the conductivity equation, $k = k_{sat}\exp[a(\theta - \theta_{sat})]$, that were considered unvarying for the whole profile. Their field measurements consisted of soil water suction recorded from tensiometers located at 30-cm depth increments for the Yolo soil. Soil water suction measurements from the tensiometers were used then with soil water characteristic curves to estimate the soil water content and the soil water flux at each soil depth. This allowed Davidson et al. (1969) to present in a figure the volumetric soil water content (θ) distribution within the Yolo loam soil (at 30, 60, 90, 120, and 180 cm depth) at various times after the cessation of infiltration without evaporation from the soil surface: 0, 1, 5, 20 and 60 days. Hereafter, we attempted to approach

1127

these field data using Kamel®, according to the characteristic information about Yolo soil described in their paper. For comparison, these soil characteristics estimated using PTFs on the basis of the texture will also be presented and used for the simulation.

3.2 Estimation of Kamel® parameters

A complete soil physical characterization requires the measurement in laboratory of the four characteristic curves mentioned above: shrinkage curve (Eq. 5), water potential curves (Eqs. 7 and 8), conductivity curve (Eq. 12) and the time dependent swelling curve (Eq. 13). These measurements may not be always available. In these cases, approximate non ideal characterization must be developed using readily available data from soil maps or any laboratory measurements on local soil samples. KamelSoil® was developed using Excel® to provide the hydrostructural parameters required by Kamel® (parameters of equations listed in Table 2) using classical soil characteristics and PTFs. Two successive steps are considered in the Kamel® parameters estimation:

1. Estimation of the hydrostructural soil state parameters provided by both equations of state of the pedostructure: the shrinkage curve and the potential curve.

2. Estimation of the dynamical parameters: of the hydraulic conductivity inter-aggregates (k_{maM}, k_{ma^o}, α_M and α^o); and of the swelling of the clayey plasma: $t_{1/2}$.

3.2.1 Hydrostructural equilibrium state parameters

They are all provided by the shrinkage curve and the water potential curve, from saturation up to the dry state. Concerning the water potential measurement, the methods of reference in laboratory that will be considered valid are the tensiometer method from saturation to 60 kPa and the Richards apparatus for suctions of 100 kPa to 1500 kPa.

There are three characterization cases: 1) the shrinkage curve and the potential curve are both available 2) only the tensiometric curve is available and 3) neither the

shrinkage curve nor tensiometric curve is available.

The ShC and the tensiometric curves were measured

The ideal scenario in this case is that the two curves were measured simultaneously on the same undistorted sample (or on two separate replicates) and that all the shrinkage phases are clearly distinguished on the shrinkage curve. The following parameters for the micro pore system (V_A, k_N, W_N), and the interpedal pore system (K_{bs}, k_M, W_M, k_L, W_L), respectively, are determined on the measured ShC, using the procedure described in Braudeau et al. (2004a). The tensiometric curve will be used for determining E_{ma}, E_{mi}, σ and W_{sat}, the water content at saturation (zero suction) by fitting equations of h_{mi} and h_{ma} on the measured curve, using Eqs. (7) and (8) where W_{mi} and W_{ma} are calculated using parameters of the ShC, namely, k_N, W_N, k_M, and W_M (Appendix A).

However, another procedure must be considered for calculating the macropore system parameters if only the micro parameters: $\overline{V}_A$, k_N, W_N, and K_{bs} can be determined or are valid using the ShC. This is the case when the ShC measurement was made on reconstituted samples (disturbed structure). In this case, the tensiometric curve is used for determining macro-parameters of the ShC: W_M, k_M, W_{sat} (at $h_{ma}=0$) along with those of the potential curve: E_{ma}, E_{mi} and σ. This is done using the Excel® solver by fitting the two equations of h_{mi} and h_{ma} (Eqs. 7 and 8) simultaneously on the measured curve (Fig. 6a). The following constraints: k_N and W_N known, $h_{mi}=h_{ma}$ over the range of 0 to 150 kPa, $h_{mi}=h_{ma}=h$ in the range of 0 to 50 kPa (validity of the measured tensiometric curve $h(W)$) are enough to get these 6 parameters above.

KamelSoil® uses this latter procedure in all cases (good measurement of ShC or not) for determining the macropore system parameters from a set of (W, h) data that may come from measurements or from estimation using pedotransfer functions (e.g. Saxton and Rawls, 2006). An Excel® sheet also is attributed to the treatment of a set of (W, V) data from the ShC measurement for estimating the shrinkage curve parameters: V_A, W_N, k_N, K_{bs}.

1129

The tensiometric curve is only available

The treatment of the tensiometric curve provides the macro pore parameters (W_M, k_M, W_{sat}, E_{ma}, E_{mi} and σ as we have seen above. Three additional inputs are required for calculating the other parameters; they can be found in soil database or estimated from texture and organic matter using appropriate pedotransfer functions (PTFs):

1. The bulk density of the pedostructure: DBD (dry) or BD (moist), corresponding to the specific volume at dry state or moist state: $\overline{V}_A = 1/DBD$ or $\overline{V}_D = 1/BD$. If DBD or BD are given, their value are put in the input Data sheet of KamelSoil®; if not, the moist bulk density BD is estimated by KamelSoil® using PTFs via θ_{sat} (or W_{sat}) and the density of the solid phase supposed equal to 2.65, according to the following equation:

$$1/BD = 1/2.65 + W_{sat} = 1/2.65 + \theta_{sat}/BD \tag{20}$$

2. The wilting point W_{1500} (soil moisture at 1500 kPa) for estimating W_N and k_N using the tensiometric curve and assuming that this point W_{1500} corresponds to the air entry point W_B on the ShC (Braudeau et al., 2005). The equations used are:

$$1500 = E_{mi}/(W_{1500} - W_N) - E_{mi}/(W_M - W_N) \tag{21}$$

and

$$k_N = 3.46 L n(2)/(W_{1500} - W_N) \tag{22}$$

according to, respectively, Eq. (8) and the relationship Eq. (22) given by Braudeau et al. (2004a) where $W_B = W_{1500}$ and $h = 1500$ kPa.

In general, the wilting point is measured in kg/kg and is available in soil data bases. In this case the gravimetric value kg/kg is put in the Data input sheet of KameSoil®. If W_{1500} is not available, KameSoil® will calculate it using the pedo-transfer functions of Saxton and Rawls (2006).

3. The standard COLE index (NRCS, 1995) for calculating $\Delta V = V_{M'} - V_{N'}$ then K_{bs}, the slope of the basic shrinkage phase of the shrinkage curve, according to the relationship $K_{bs} = (\overline{V}_{M'} - \overline{V}_{N'})/(W_M - W_N)$ (Appendix A). The COLE denotes the fractional change in the clod dimension from a dry to a moist state at 33 kPa. It can be expressed such as:

$$\text{COLE} = (\overline{V}_{33}/\overline{V}_{Dry})^{1/3} - 1 \approx (\overline{V}_{33} - \overline{V}_{Dry})/(3\overline{V}_{Dry})$$

Assuming that $\overline{V}_{33}$ is a good approximation of $\overline{V}_{M'}$ for all types of ShC (Fig. 3) and that $\overline{V}_{dry} = \overline{V}_{N'} = \overline{V}_A$, we can then calculate K_{bs} as:

$$K_{bs} = (3\text{COLE}\overline{V}_D/(3\text{COLE} + 1))/(W_M - W_N) \tag{23}$$

If the COLE index is not available, a relationship between K_{bs} and the contents in clay, silt and sand (kg/kg) can be sought (Braudeau et al., 2004b, Boivin et al., 2004). In KamelSoil® Eq. (24) is used waiting for more investigations:

If $(\text{Clay} + 0.25\text{Silt}) > 0.5$ kg/kg then $K_{bs} = 1.1$ else $K_{bs} = 2(\text{Clay} + 0.25\text{Silt})$ (24)

Both shrinkage and tensiometric curves are not available

In addition to the three soil properties listed in the section above (*BD, W_{1500}, COLE* or K_{bs}) two other properties are required 1) the soil moisture at 100 kPa (1 bar), W_{100} and 2) soil moisture at 33 kPa: W_{33}. These characteristics are generally measured and found in the soil data bases in kg/kg. If not, they will be estimated in KamelSoil® using pedotransfer functions according to Saxton and Rawls (2006). With W_{1500}, and W_{33}, one can calculate the two parameters A and B of the Eq. (25) used by Saxton and Rawls (2006) for representing the tension segment of 1500 to 33 kPa:

$$h_{(1500-33)} = A W^B \tag{25}$$

In KamelSoil® this equation is used to fit h_{mi} (Eq. 8) on these three points (W_{1500}, W_{100} and W_{33}) and on h_{ma} (Eq. 7) between 100 kPa to saturation (0 kPa). The assumption here is that h_{mi} and h_{ma} are equal from 70 kPa up to saturation, which is the case for many soils. Thus, the segment between 33 kPa and saturation which was taken as

5 a straight line by Saxton and Rawls (2006) is actually modelled by h_{ma} and h_{mi} under this assumption Fig. 6b. This procedure provides W_M, k_M, W_{sat}, E_{ma}, σ, E_{mi}, W_N, and k_N.

3.2.2 Hydrostructural dynamic parameters

Parameters of $k_{ma}(W_{ma})$ in Eq. (12) are estimated by fitting this equation to the con-
10 ductivity curve $k(\theta)$ simulated by Brooks and Corey equation (1964):

$$k(\theta) = k_{sat}((\theta - \theta_r)/(\phi - \theta_r))^n \tag{26}$$

where parameters θ_r and n are determined by PTFs from clay %, sand %, and poros-
ity ϕ (volume fraction) according to Saxton and Rawls (2006). The conductivity at
saturation k_{sat} is calculated by the Saxton and Rawls (2006) procedure according the
15 following relationship:

$$k_{sat} = 1930(\theta_{sat} - \theta_{33})^{(3-1/B)} \tag{27}$$

where B is the parameter of Eq. (25) calculated with points (W_{1500}, 1500 kPa) and (W_{33}, 33 kPa).

The conductivity equation of Kamel® (Eq. 12) is then adjusted to the conductivity
20 curve of Brooks and Corey (1964) (Eq. 26) using the solver function of Excel® after
initialization of the Kamel® parameters as:

$$\alpha_M = n/(W_{sat} - W_N); k_{ma^o} = k(\theta_C); k_{maM} = k(\theta_M) \tag{28}$$

and α_o given by Eq. (12) at $W = W_M$ ($k_{ma} = k_{maM}$ and $W_{maM} = w_{st}(W_M) = -Ln(2)/k_M$ from Eq. (A2) of w_{st} in Appendices).

An example is presented on Fig. 7a showing the fit of the logistic equation of k_{ma} on the conductivity curve estimated by KamelSoil® from the texture for two horizons of the Yolo loam soil which is studied here after. For comparison, we put on Fig. 7b the measured corresponding data (Davidson et al., 1969) fitted also by the logistic equation of k_{ma}. This procedure was automated in KamelSoil®.

Concerning the absorption rate of water by the swelling plasma of primary peds, k_{mi}, this rate was rarely measured. The time of half charge, $t_{1/2}$, which is chosen as parameter for representing k_{mi} via Eq. (14), depends on the soil plasma and its degree of division in the structure. It was fixed at 30 min, waiting for more future investigations.

4   Results and discussion

4.1   Parameters estimation using measured soil characteristics

4.1.1   Soil water pools and water potential parameters

The potential curve is measured, from 0 to 50 kPa, while the shrinkage curve was not measured. Based on soil texture of 18% clay, 49% silt and 33% sand found in literature for the Yolo Loam Soil, KamelSoil® calculates W_{1500} for the four depths of which the bulk density is, respectively: 1.36, 1.17, 1.8, 1.17. That gives, respectively W_{1500}=0.086 at 30 cm and 0.10 at 60; 90 and 120 cm. These values were used as approximate values of W_B to calculate W_N and k_N. As in KamelSoil®, all parameters of W_{ma}, h_{ma} and h_{mi} (W_M, k_M, W_{sat}, E_{ma}, σ, E_{mi}, k_N and W_N) were determined by optimizing the fit of both h_{mi} and h_{ma} on the ten points (W, h) of the potential curve measured by Davidson et al. (1969) and the point (W_{1500}, 1500 kPa) estimated above. Results are presented in Table 3 for the four horizons considered by Kamel®.

For comparison, the potential curves of the four horizons were estimated using KamelSoil® from the texture according to the pedotransfer functions proposed by Saxton and Rawls (2006), except for the bulk density which was given. Estimated pa-

rameters are listed in Table 4 and Fig. 8a shows the potential curves of two horizons measured (Davidson et al., 1969) and estimated according to the pedotransfer functions.

4.1.2 Hydraulic conductivity parameters

Davidson et al. (1969) observed that their field measurements of water potential and fluxes at the various depths fitted very well to the following exponential equation:

$$k = k_o \exp(a(\theta - \theta_o)) \tag{29}$$

where θ is the volumetric water content, $k_o = 50$ cm/day, $a = 48.2$ cm$^3_{\text{soil}}$/cm$^3_{\text{water}}$ and $\theta_o = 0.474$ cm$^3_{\text{water}}$ cm$^{-3}_{\text{soil}}$ for all depths of the Yolo loam soil.

As for estimation of the conductivity parameters using KamelSoil®, we searched the better fit of Eq. (12)–(29) measured by Davidson et al. (1969) using the solver of Excel® as follows:

In first approximation, parameters of Eq. (12) are estimated considering the high and low ranges of W_{ma} as in the Appendix B:

$$\rho_w \, \alpha_M = aBD \tag{30}$$

$$k_{maM} = k_o \exp(\alpha_M W_M - a\theta_o) \tag{31}$$

$$k_{ma^o} = k(\theta_C) = k_o \exp(\alpha_M W_C - a\theta_o), \tag{32}$$

the conductivity at point C, where W_{ma} is near 0.

The fourth parameter α_o is estimated by equating Eqs. (12) and (31) at $W = W_M$, knowing that $W_{maM} = -\ln(2)/k_M$ according to Equation of $W_{ma} = w_{st} + w_{ip}$ in Table 2:

$$\alpha_o = \frac{1}{W_{maM}} \ln \left(\frac{k_{maM}/k_{ma^o}}{1 - \exp\left(-\alpha_M W_{maM}\right)} \right). \tag{33}$$

Excel[®] solver is then used for optimizing the fit by changing ($10^{11}\alpha_0$), ($10^8\alpha_M$), k_{ma^o} and k_{maM}. Results are presented together with those calculated using KamelSoil[®] from the texture, bulk density and W_{sat}, on Fig. 8b. We note that a very good fit of the Kamel[®] Eq. (12) on the exponential Eq. (29) of Davidson's data (straight line) and the important difference between these data and the hydraulic conductivity estimated by KamelSoil[®] using Brooks and Corey Eq. (26) with pedotransfer functions.

4.1.3 Determination of K_{bs}, V_A and $t_{1/2}$

K_{bs} was estimated near $0.6\,\mathrm{dm^3/kg}$ by KamelSoil[®] for this loam soil according to Eq. (24).

In order to calculate the lower value of the specific volume, V_A, it is assumed that the soil bulk density considered by Davidson et al. (1969), as well as bulk density estimated by Saxton and Rawls (2006) using pedotransfer functions, is the bulk density at field capacity, ($1/\overline{V}_D$). Then the pedostructure specific volume at dry state is:

$$\overline{V}_A = \overline{V}_D - K_{bs}(W_M - W_N) \tag{34}$$

This completes the parameters needed to construct the shrinkage curve including: $\overline{V}_A$, K_{bs}, W_N, k_N, W_M, k_M, and W_{sat} (with k_L=100). The last parameter required, the half time of swelling $t_{1/2}$, was fixed to 30 min, mean value of the results given by Braudeau and Mohtar (2006).

4.2 Simulation of field experiments

Tables 3 and 4 summarize the fifteen required pedostructure parameters for Kamel[®] that were calculated, respectively, from the soil data of Davidson et al. (1969) and those estimated using KamelSoil[®]. In Table 3, parameters that do not correspond to any measurement are only K_{bs}, W_N, k_N and $t_{1/2}$ which concern the micropore system

behavior. The thicknesses of horizons were not given in the article; they were taken for the simulations as 0–40, 40–80, 80–100, and 100–120 cm.

Figure 9 shows the computed moisture profiles of Kamel® at 0, 1, 5, 20, and 60 days of drainage, without evaporation from the surface and starting from the saturated state after infiltration. For comparison, the field measured data of Davidson et al. (1969) are shown on the figure: the soil water content at 30, 60, 90 and 120 cm depth after 1 day, 5, 20 and 60 days of drainage without evaporation. Non calibrated simulation results have a good agreement with measured values (Fig. 9a): the first day, $\Delta W_{1\text{day}}=-0.006$ and $0.02\,\text{kg/kg}$ are the water content at 60 and 120 cm, respectively. Less than 0.01 kg/kg are observed at 5 and 20 days for horizons 3 and 4 (90 and 120 cm).

Assuming that parameters of the hydraulic conductivity are responsible of these little deviations we tried to change the input values of W_{sat} (corresponding to the term θ_o in Eq. 29) of horizons 2 and 4, adding to W_{sat} the observed deviation between the measured and simulated water content at one day: -0.006 and $0.02\,\text{kg/kg}$, respectively. The new simulation showed on Fig. 9b reproduces exactly all the experimental field data except the very light deviation ($-0.004\,\text{kg/kg}$) observed for the water contents of horizons 2 and 3 at 60 days. In fact, because of the relationship between k_o and θ_o in Eq. (29), leading to Eq. (B10) in the Appendix B relating the hydraulic conductivity parameters between them, the same effect on the simulation is obtained by changing k_{sat} instead of W_{sat} according to:

$$k'_{\text{sat}} = k_{\text{sat}}\exp\left(-\alpha_M \Delta W_{1\text{day}}\right) \tag{35}$$

The new values of k_{sat}, $k'_{\text{sat}}=3.9\times10^{-4}$ and 8×10^{-5}, instead of the common value of 2.6×10^{-4} for both horizons 2 and 4, keep the conductivity curves within the cloud of experimental data reported in the graph ($\log(k)$ vs. θ) used by Davidson et al. (1969) for determining parameters of the unique exponential Eq. (29) that they proposed for the whole soil profile. This simplistic procedure of calibration, used for approaching the accurate values of the conductivity parameters, is justified in Appendix C according to

the equation of the water content developed by Davidson et al. (1969) at depth L and time t after the end of the infiltration while the hydraulic gradient is near unity.

For comparison, we present in Fig. 10a the simulation of the same field experiment but using the soil parameters estimated by KamelSoil® from texture data only. Results are coherent but very different from the measured field data. We applied the same procedure listed above for correcting the hydraulic conductivity: new values of k_{sat} were calculated using Eq. (35) where ΔW_{1day} had the observed values 0.009, 0.015 and 0.036 kg/kg for horizons 2, 3 and 4; that gave a new k_{sat} of 1.3×10^{-4}, 8.5×10^{-5} and 3.6×10^{-5}, respectively. The new simulation presented on Fig. 10b provided much better results. The deviation observed at 60 days comes certainly from the slopes, represented by the coefficient α_M (Tables 3 and 4), of the estimated conductivity curves of the last horizons which are lower than those of the measured ones (see Fig. 8b).

These results demonstrate that in the range of the water contents obtained by drainage (without water uptake by plants), the exponential equation proposed by Davidson et al. (1969) seems to be the physical adequate equation for the hydraulic conductivity of a soil, at least in the range of 0 to 20 kPa. Several works assumed this shape of equation for developing useful methods for determining the hydraulic conductivity function in spite of the uncertainty of the measurement and model (Libardi et al., 1980; Wendroth et al., 1993b; Reichardt et al., 2004); despite the fact that no pedotransfer function were introduced using this form of equation. The three parameters k_o, a, and θ_o, reduce in fact in two characteristic parameters: $k_o/\exp(a\theta_o)$ and a, that are constant within the profile regardless the very different bulk density of the first horizon. They seem to be characteristic of the soil material, independent of changes in bulk density. The fact that using W_{ma} instead of the total water content W in the conductivity equation highlight Eqs. (B9) and (B10) developed in the Appendices between conductivity parameters (α, α_M, a, θ_o, k_o, k_{sat}, k_{maM}) of both exponential equations (in terms of water content and water suction) and some parameters of the pedostructure such as E_{ma}, W_M, W_{sat}, and V_D.

Notably, knowing that α_M is of the form $\alpha_M = a'/\overline{V}$, where a' is a constant similar to a

characteristic of the material regardless to the structure, is important for the determination of this parameter and research of related pedotransfer functions. Results in Table 4 give $a'=\alpha_M/BD=57\pm1$ for this loam soil. In the same way, k_{sat} must be measured or found in databases along with the corresponding value of W_{sat} since the characteristic

5 of the curve is k_{sat}/W_{sat}.

Concerning the two other parameters, k_{ma^o} and α^o, they cannot be commented on because they have no impact within the range of water content covered by the field experiment. It is the same for functionalities of Kamel[®] relative to the dynamic of swelling of the primary peds, such as the water exchange between both macro and

10 micro pore systems and the aperture of fissures or cracks with drying.

Overall, this example demonstrates that the use of Kamel[®] for simulating the soil and water can be easily and accurately adapted according to the degree of information available at our disposal.

It is important to note that if these parameters have been measured in laboratory,

15 then in theory the model does not need to be calibrated because the 4 basic functions of a soil horizon (shrinkage curve, soil water potential curve, hydraulic conductivity curve and the time dependent swelling curve) would have already been determined. In contrary, if only the texture is known, then KamelSoil[®] estimates the 15 characteristic parameters of the soil with a degree of approximation depending on the pedotransfer

20 functions used. Hence, the result of the simulation will be coherent but approximate; and modeling by Kamel[®] may require calibration with field data like other soil-water models. Nevertheless, for Kamel[®], knowledge of the physical significance of the parameters describing the four characteristic functions of the pedostructure simplifies this calibration step as this has been showed in the case of the saturated hydraulic conduc-

25 tivity (Appendix C), which no longer requires a long and difficult sensitivity analysis as in the case of other models.

5 Conclusions

We have shown a new paradigm for soil water modeling that is built on new concepts of Structure Representative Elementary Volume (SREV) and pedostructure that takes into account the hierarchical internal organization of the soil medium. The paper also demonstrated the paradigm to ensure the transfer of scale from laboratory characterization to soil water modeling at the field level. A computer model Kamel® was developed based on this theory.

As a soil-structure water model, Kamel® has the following features:

1. It represents the soil organizational characteristics and variables for each hydrostructural state at any soil depth.

2. It is able to simulate the water flow in this organization (the vadoze zone) in response to external factors such as rain, ETP (inducing water uptake by roots), and structural change of the surface layer.

3. It generates outputs which keep the link between the internal physical state variables (SREV variables, referred to the structural mass of solids and used for describing processes at their local scale) with the classical volumetric averaged variables used in agriculture to generalize at larger scales (REV variables, units in dm/dm or kg/ha). The model therefore solves the scaling problem among measurements in laboratory, estimation from soil databases, and modeling at the field scale.

4. It allows as a framework to integrate biogeochemical processes that act at the pedostructure level.

Because Kamel® is entirely founded on physical equations describing the soil-water interaction, and on significant and measurable parameters, it can be adapted to all types of soil and situations (simulation of experiments in the laboratory or in the field).

1139

In particular, it is able to provide the same macroscopic information (volumetric variables) as that commonly sought after using existing soil-water models and the characteristics inputs of these models, which are often estimated by pedotransfer functions. But, at the same time, it also describes the internal functioning of the corresponding pedon as if it was characterized by the 15 pedostructure parameters. For this, it relies on a program associated to Kamel®, KamelSoil, which transforms common information generally used today to characterize soils (texture, pF4,2, apparent density, . . .) into the set of hydrostructural parameters needed for Kamel using pedotransfer functions.

For all these reasons Kamel® can be used as a standard reference to evaluate other soil-water models and also pedotransfer functions at a given location or agronomical situation.

Appendix A

Water pools equations

At equilibrium at given water content W, equations of the water pools in term of the total water content W are, according to Braudeau et al., 2004a:

$$w_{ip}^{eq} = \frac{1}{k_L} ln[1 + \exp(k_L(W - W_L))] \tag{A1}$$

$$w_{st}^{eq} = -\frac{1}{k_M} ln[1 + \exp(-k_M(W - W_M))] - w_{ip}^{eq} \tag{A2}$$

$$w_{bs}^{eq} = \frac{1}{k_N} ln[1 + \exp(k_N(W - W_N))] + \frac{1}{k_M} ln(1 + \exp(-k_M(W - W_M))) \tag{A3}$$

$$w_{re}^{eq} = -\frac{1}{k_N} ln[1 + \exp(k_N(W - W_N))] + W \tag{A4}$$

1140

Parameters W_N, W_M, W_L are the water content at the intersection points N′, M′, L′ of the tangent lines extending the quasi-linear shrinkage regions of the shrinkage curve (Fig. 3). Their values represent characteristic pore volumes of the pedostructure with ρ_w being the water density in $kg\,dm^{-3}$:

5   $W_N = \max(w_{re}) = \rho_w \min(Vp_{mi})$, the pore specific volume of primary peds at dry state;
$W_M = \max(w_{re}) + \max(w_{bs}) = \rho_w \max(Vp_{mi})$, the maximum pore specific volume of saturated primary peds; and

$W_L - W_M = \max(w_{st}) \approx \rho_w Vp_{ip}$, the interpedal pore specific volume in the structural linear region of the shrinkage curve (D–E).

10   Parameters k_N, k_M, and k_L represent the y-distance between these intersection points and the shrinkage curve (as for example: $k_M/\mathrm{Log}\,2 = (K_{bs} - K_{st})/(V_M - V_{M'})$). They are constants under experimental conditions, but they depend on the load and overburden pressure under field conditions.

Appendix B

15

The conductivity curve equation

In the literature, the hydraulic conductivity is expressed in terms of the suction h rather than W. Many authors cited by Angulo-Jamarillo et al. (2000) used the exponential expression of k in terms of the soil water suction h (Eq. 6, Gardner, 1958) in deterministic
20   models and in particular for the in situ measurement of conductivity using disc or ring infiltrometers:

$$k = k_{\mathrm{sat}}\exp(\alpha h) \tag{B1}$$

where k_{sat} is the apparent field saturated hydraulic conductivity and α is a constant.

We note that for high water content, Gardner's equation above can be written in
25   terms of W_{ma}. Indeed, according to Eq. (7), the suction pressure h_{ma} for the high range

of water contents can be expressed such as:

$$h_{ma} = \frac{\rho_w E_{ma}}{W_{maSat} + \sigma} \left(\frac{1}{\Delta W_{ma}/(W_{maSat} + \sigma) + 1} - 1 \right) \approx \frac{\rho_w E_{ma}}{W_{maSat}^2} (W_{maSat} - W_{ma}) \quad \text{(B2)}$$

Substituting h in Eq. (B1) by h_{ma} leads to:

$$k = k_{sat}\exp(\alpha_M(W_{ma} - W_{maSat})) = k_{maM}\exp(\alpha_M W_{ma}) \quad \text{(B3)}$$

where $\alpha_M = -\alpha\rho_w E_{ma}/(W_{maSat})^2 > 0 \quad \text{(B4)}$

and $k_{maM} = k_{sat}/\exp(\alpha_M W_{maSat}) \quad \text{(B5)}$

Finally, knowing that $W_{ma}=W-W_{mi}$ and that $W_{mi} \approx W_M$ (Appendix A) in the high range of water content, the hydraulic conductivity in the range of water content near saturation (Eqs. B1 and B3) can also be written in terms of W such as:

$$k = k_{sat}\exp(\alpha h) = k_{maM}\exp(\alpha_M W_{ma}) = [k_{maM}/\exp(\alpha_M W_M)]\exp(\alpha_M W) \quad \text{(B6)}$$

The same for Eq. (B5) leads to:

$$k_{maM}/\exp(\alpha_M W_M) = k_{sat}/\exp(\alpha_M W_{sat}) \quad \text{(B7)}$$

These Eqs. (B6) and (B7) match very well with the following conductivity equation that was found by Davidson et al. (1969) from their field experimental data:

$$k = k_o\exp(a(\theta - \theta_o)) \quad \text{(B8)}$$

where θ is the volumetric water content and k_o, a, θ_o are soil characteristics. k_o and θ_o are the hydraulic conductivity and the corresponding water content at a point in high range of moisture. Identifying Eqs. (B6) and (B8) and using Eqs. (B4) and (B5) leads to:

$$a = \alpha_M\rho_w/BD = \left(-a\rho_w^2 E_{ma}/BD\right)/(W_{sat} - W_M)^2 \quad \text{(B9)}$$

where BD is the bulk density at moist state, and

$$k_o/\exp(a\theta_o) = k_{sat}/\exp(\alpha_M W_{sat}) = k_{maM}/\exp(\alpha_M W_M) \quad \text{(B10)}$$

1142

Appendix C

Calibration of k_{sat}

The procedure used for correcting k_{sat} can be justified as follows, according to equations developed by Davidson et al. (1969): up until the first day after infiltration water drains under a unit hydraulic gradient and in a relatively uniform soil profile Black et al. (1969) shown that the hydraulic conductivity should increase with soil depth after the cessation of infiltration as:

$$k(z) = v_L z/L \tag{C1}$$

where L is the length (dm) of the drainage profile and v_L is the soil-water flux (dm/s) at L. Introducing k in the continuity equation leads to:

$$dW/dt = -\rho_w \overline{V} dk/dz = -\rho_w \overline{V} v_L/L = (\rho_w/BD)k/L \tag{C2}$$

Using our terminology, for high water contents, $W = W_{ma} + W_{mi} = W_{ma} + W_M$ and $k_{ma} \, (\equiv k)$ can be approximated by, according to Eqs. (B6) and (B7):

$$k_{ma} = k_{maM}\exp(\alpha(W - W_M)) = k_{\text{sat}}\exp(\alpha(W - W_{\text{sat}})) \tag{C3}$$

After substitution in Eq. (C2) and integration with time leads to:

$$W = W_{\text{sat}} - \frac{1}{\alpha}\ln(1 + \alpha k_{\text{sat}}t/L) \tag{C4}$$

Thus, a deviation of $\Delta W = W_1 - W_2$ at time t and depth L corresponds to $\Delta k_{\text{sat}} = k_{sat1} - k_{sat2}$ such that:

$$\exp(-\alpha\Delta W) = (1 + \alpha k_{sat1}t/L)/(1 + \alpha k_{sat2}t/L) \tag{C5}$$

Since the term $(\alpha k_{\text{sat}}t/L)$ is larger then 1 (at $t = 8640$ s), Δk_{sat} can be approximated by:

$$k_{sat1} = k_{sat2}\exp(-\alpha_M(W_1 - W_2))$$

1143

Appendix D

Kamel[®] model Simile[®] version

The Kamel[®] model was developed in the Simile[®] (http://www.simulistics.com) environ-
ment by Braudeau (2006) according to the concepts and equations presented in the
article. Nomenclature, equations and parameters are listed in Tables 1 and 2.

The model is composed of three parts (input, output and pedon), which are described
below.

a) Inputs: Four kinds of input are shown as submodels:

Pedon parameters (fixed parameters) comprising the depths of the four soil horizons,
the thickness of the soil layers (choice of the discretization), the root distribution (% of
the total roots mass) by horizon, and the *pedostructure* parameters for each horizon,
that says the parameters of the four characteristic curves.

Initial soil moisture (fixed parameter) which consists of initial saturation level of the
available water in each soil layer along the profile.

Rain and/or evapotranspiration (variable parameters) for entering the potential
evapo-transpiration and rain intensity during simulation.

Surface properties and end-of-profile drainage conditions (variable parameters) giv-
ing the conditions at the surface and the end of the profile. Some properties of the
surface layer (for example, conductivity at saturation, specific volume, thickness of the
surface layer, and surface water storage) can be changed during a simulation taking
into account the impact of tillage, irrigation, etc. The condition at the end of the profile
concerns the drainage, which can be either free or sealed drainage.

b) Output: The different kinds of output are:

State variables in the SREV units at 10 cm depth increments from the surface.

Volumetric contents (REV variables) of water pools, pore space, air, available water
storage, available macropore water storage, etc. per group of 1 dm of soil layers over
the entire soil profile.

Local state variables in the SREV units of a soil layer (2 cm thick) at a chosen depth. The variables of this submodel can be displayed in xy graphs, such as $h_{ma}=f(W)$ or $W_{ma}=f(W)$.

All state variables of the surface referenced to the structural mass of the surface layer. These variables can also be displayed in xy graphs.

All variables of the soil profile water budget, such as infiltration (cumulative flux trough the first layer), drainage (through the last layer), runoff, water storage in the profile, water storage in the surface layer and on the surface, and rain.

c) Pedon: The pedon is presented as a stack of soil-layers: each layer contains the same mechanism (equations, compartments, flux, variables) with variables and parameters having their own values according to the layer position in the stack. Each layer is in relationship with its adjacent layer above and below by means of two associations with a submodel outside the pedon submodel.

A soil layer is organized into seven sub-units (except for the first layer, which has one additional surface unit). These sub-units are similar to directories containing variables, parameters, fluxes, and compartments, which can be inspected at any time by pointing the cursor to the particular variable:

- *Horizon parameters*: the input pedohydral parameters are distributed by horizon for each layer.

- *Water fluxes*: The two fluxes are computed for each time step, F_1 flux through the upper surface of the layer and F_2 flux through the lower surface.

- *Layer state variables*: This submodel calculates the changes in W and W_{mi} due to net flux (F_2-F_1) (see Fig. 5) and to the resulting change in water potential ($h_{mi}-h_{ma}$) between the two compartments, respectively. Then, $W_{ma}=W-W_{mi}$ is calculated along with all the state variables of the layer.

- *Cell size*: The dimensions of a pedostructure unit in which H_i is the height of the layer are calculated at the field capacity point (W_D). Point D corresponds

to the maximum swelling of the pedostructure and is taken as reference since it is assumed that for $W > W_D$, the structural volumes of the layer and of the pedostructure are equal. The horizontal dimensions, a and b, are not defined in this one-dimensional simulation.

- – *Initial W and W_{mi}*: The two variables representing initial soil water (W) and initial water in micropores (W_{mi}) are calculated from a given hydral state profile as input. They constitute the initial values of the two corresponding compartments W and W_{mi} in the *State variables of each layer* submodel.

- – *Volumetric state variables*: The SREL organizational variables which are calculated in kg or dm^3 per kg of solids are converted in volumetric variables (in dm per dm of soil height or in kg per dm^3 of soil) for each layer.

- – *Water balance terms*: The total water inputs and outputs and the water storage in the pedon are calculated in this submodel.

- – The *Surface variables* submodel is also updated at each time step. Their changes in value result from the water balance between the flux into the first layer, the rain, runoff, and the change in the water storage into and above the surface layer.

References

Angulo-Jamarillo, R., Vandervaere, J. P., Roulier, S., Thony, J. L., Gaudet, J. P., and Vauclin, M.: Field measurement of soil surface hydraulic properties by disc and ring infiltrometers: A review and recent developments, Soil Till. Res., 55, 1–29, 2000.

Bear, J.: Dynamics of Fluid in Porous Media, American Elsevier, New York, p. 764, 1972.

Berezin, P. N., Voronin, A. D., and Shein, Y. V.: An energetic approach to the quantitative evaluation of soil structure, Pochvovedeniye, 10, 63–69, 1983.

Boivin, P., Garnier, P., and Tessier, D.: Relationship between clay content, clay type, and shrinkage properties of soil samples, Soil Sci. Soc. Am. J., 68, 1145–1153, 2004.

Braudeau, E.: Kamel Simile version, Agence pour la Protection des Programmes, Paris, IDDN.FR.001.390019.000.S.P.2006.000.31500, 2006.

Braudeau, E. and Bruand, A.: Détermination de la courbe de retrait de la phase argileuse à partir de la courbe de retrait établie sur échantillon de sol non remanié, C.R. Acad. Sci. Paris, 316(II), 685–692, 1993.

Braudeau, E. and Mohtar, R. H.: Modeling the Soil System: bridging the gap between pedology and soil-water physics, Global Planet. Change J., accepted, doi:10.1016/j.gloplacha.2008.12.002, 2009.

Braudeau, E. and Mohtar, R. H.: Modeling the swelling curve for packed soil aggregates using the pedostructure concept, Soil Sci. Soc. Am. J., 70, 494–502, 2006.

Braudeau, E. and Mohtar, R. H.: Water potential in non rigid unsaturated soil-water medium, Water Resour. Res., 40, W05108, doi:10.1029/2004WR003119, 14, 2004.

Braudeau, E., Frangi, J. P., and Mothar, R. H.: Characterizing non-rigid dual porosity structured soil medium using its shrinkage curve, Soil Sci. Soc. Am. J., 68, 359–370, 2004a.

Braudeau, E., Mohtar, R. H., and Chahinian, N.: Estimating soil shrinkage parameters, in: Development of pedotransfer functions in soil hydrology, edited by: Pachepsky, Y. and Rawls, W., Elsevier, Amsterdam, 225–240, 2004b.

Braudeau, E., Sene, M., and Mohtar, R. H.: Hydrostructural characteristics of two African tropical soils, Eur. J. Soil Sci., 56, 375–388, 2005.

Brewer, R.: Fabric and Mineral Analysis of Soils, John Wiley and Sons, New York., 482 pp., 1964.

Brooks, R. H. and Corey, A. T.: Hydraulic properties of porous media, Hydrology paper No. 3, Colorado State University, Fort Collins, USA, 1964.

Bruckler, L., Bertzzi, P., Angulo-Jamarillo, R., and Ruy, S.: Testing an infiltration method for estimating soil hydraulic properties in the laboratory, Soil Sci. Soc. Am. J., 66, 384–395, 2002.

Chen, C., Thomas, D. M., Green, R. E., and Wagenet, R. J.: Two-domain estimation of hydraulic properties in macropore soils, Soil Sci. Soc. Am. J., 57, 680–686, 1993.

Colleuille, H. and Braudeau E.: A soil fractionation related to soil structural behavior, Aust. J. Soil Res., 34, 653–669, 1996.

Davidson, J. M., Stone, L. R., Nielson, D. R., and Larue, M. E.: Field measurement and use of soil water properties, Water Resour. Res., 5, 1312–1321, 1969.

5 Gerke, H. H. and van Genuchten, M. T.: A dual-porosity model for simulating the preferential movement of water and solutes in structured porous media, Water Resour. Res., 30, 1945–1954, 1993.

Katterer, T., Schmied, B., Abbaspour K. C., and Schulin, R.: Single- and dual-porosity modelling of multiple tracer transport through soil columns: Effects of initial moisture and mode of application, Eur. J. Soil Sci., 52, 25–36, 2001.

10 Libardi, P. L., Reichardt, K., Nielson, D. R., and Biggar, J. W.: Simple field method for estimating soil hydraulic conductivity, Soil Sci. Soc. Am. J., 44, 3–7, 1979.

Logsdon, S. D.: Determination of preferential flow model parameters, Soil Sci. Soc. Am. J., 66, 1095–1103, 2002.

15 Low, P. F.: Structural component of the swelling pressure of clays, Langmuir 3, 18–25, 1987.

Mohtar, R. H., Jabro, J. D., and Buckmaster, D.: Field testing of the grazing simulation model: GRASIM, Trans. ASABE, 40, 1495–1500, 1997.

McIntyre, D. S., Watson, C. L., and Loveday, J.: Swelling of a clay soil profile under ponding, Aust. J. Soil Res., 20, 71–79, 1982.

20 National Resources Conservation Service: Soil Survey Laboratory Information Manual, Soil Survey Investigation Report no. 45, National Soil Survey Center. Lincoln Nebraska, 316 pp., available at: http://soils.usda.gov/survey/nscd/lim/, 1995.

Othmer, H., Diekkrüger, B., and Kutilek, M.: Bimodal porosity and unsaturated hydraulic conductivity, Soil Sci., 152, 139–149, 1991.

25 Quirk, J. P. and Panaboke, C. R.: Incipient failure of soil aggregates, J. Soil Sci., 13, 60–70, 1962.

Reichardt, K., Timm, L. C., Bacchi, O. O. S, Oliveira, J. C. M., and Dourad-Neto, D.: A parameterized equation to estimate soil hydraulic conductivity in the field, Aust. J. Soil Res., 42, 283–287, 2004.

30 Saxton, K. E. and Rawls, W. J.: Soil water characteristic estimates by texture and organic matter for hydrologic solutions, Soil Sci. Soc. Am. J., 70, 1569–1578, 2006.

Simunek, J., Wendroth, O., Wypler, N., and van Genuchten, M. T.: Non-equilibrium water flow characterized by means of upward infiltration experiments, Eur. J. Soil Sci., 52, 13–24, 2001.

Simunek, J., Jarvis, N. J., van Genuchten, M. T., and Gardenas, A.: Review and comparison of models for describing non -equilibrium and preferential flow and transport in the vadose zone, J. Hydrol., 272, 14–35, 2003.

Stöckle, C. O., Donatelli, M., and Nelson, R.: CropSyst, a cropping systems simulation model, Eur. J. Agr., 18, 289–307, 2003.

Voronin, A. D.: A new approach to determining the dependence of the capillary-sorption potential on soil moisture content, Pochvodedeniye, No. 10, 1980.

Wendroth, O., Ehlers, W., Hopmans, J. W., Kage, H., Halbertsma, J., and Wösten, J. H. M.: Reevaluation of the evaporation method for determining hydraulic functions in unsaturated soils, Soil Sci. Soc. Am. J., 57, 1436–1443, 1993a.

Wendroth, O., Katul, G. G., Parlange, M. B., Puente, C. E., and Nielsen, D. R.: A non linear filtering approach for determining hydraulic conductivity functions in field soils, Soil Sci., 156, 293–301, 1993b.

Table 1. Pedostructure state variables. Subscripts *mi* and *ma*, *hor*, *fiss*, and *s*; refer to as micro and macro, horizon, fissures and solids; *ip*, *st*, *bs* and *re*, refer to as the name of the corresponding shrinkage phase of the shrinkage curve: interpedal, structural, basic and residual.

Volume of concern	Specific volume (dm^3/kg)	Specific pore volume (dm^3/kg)	Specific water content (kg w./kg soil)	Non swelling water (kg w./kg soil)	Swelling water (kg w./kg soil)	Suction pressure (kPa)	Conductivity (dm/s)
Horizon	$\overline{V}_{hor}$	Vp_{fiss}	W_{hor}				
Pedostructure	$\overline{V}$		W			h	k
Interpedal porosity		Vp_{ma}	W_{ma}	w_{st}	w_{ip}	h_{ma}	k_{ma}
Primary peds	$\overline{V}_{mi}$	Vp_{mi}	W_{mi}	w_{re}	w_{bs}	h_{mi}	k_{mi}
Primary particles	$\overline{V}_s$						

Table 2. Equations and parameters of water pools and hydrostructural characteristic curves of the pedostructure (soil medium).

State variable	Equation	Parameters
	Water pools equations at equilibrium state	
Interped swelling water	$w_{ip}^{eq} = (1/k_L)\, ln[1+\exp(k_L\,(W-W_L))]$	$k_L,\ W_L$
Interped Structural water	$w_{st}^{eq} = -\,(1/k_M)\, ln[1+\exp(-k_M\,(W-W_M))] - w_{ip}^{eq}$	k_M, W_M
Plasmic basic water	$w_{bs}^{eq} = (1/k_N)\, ln[1+\exp(k_N\,(W-W_N))] + (1/k_M)\, ln(1+\exp(-k_M\,(W-W_M)))$	$k_M,\ W_M,\ k_N,\ W_N$
Plasmic residual water	$w_{re}^{eq} = -\,(1/k_N)\, ln[1+\exp(k_N\,(W-W_N))] + W$	
Shrinkage curve		
Pedostructure specific volume	$\overline{V} = \overline{V}_A + K_{bs} dw_{bs} + dw_{ip}$	$V_A,\ K_{bs}$
Swelling and suction pressures curves		
Interped swelling pressure	$Ps_{ma} = \rho_w E_{ma}/(W_{ma}+\sigma)$	$E_{ma},\ \sigma,\ W_{sat},\ W_M$
Interped suction pressure	$h_{ma} = Ps_{ma} - \rho_w E_{ma}/(W_{sat}-W_M+\sigma)$	
Primary ped suction pressure	$h_{mi} = \rho_w E_{mi}\,(1/(w_{bs})-1/(W_M-W_N))$	$E_{mi},\ W_M,\ W_N$
Conductivity		
Soil conductivity for the macropore water	$k_{ma} = \dfrac{k_{maM}\exp(\alpha_o W_{ma})}{k_{maM}/k_{ma^o}+\exp((\alpha_a-\alpha_M)W_{ma})}$	$\alpha^o,\ k_{ma^o},\ \alpha_M\ k_{maM}$
Primary peds conductivity (constant)	$k_{mi} = 0.1931\,(W_M-W_N)^2/(\rho_w E_{mi} t_{1/2})$	$t_{1/2}$ (time of half charge)

1151

Table 3. Kamel® parameters calculated from the measured data of Davidson et al. (1969).

no.	Parameters	horizon1	horizon2	horizon3	horizon4	Units
1	K_{bs}	0.6	0.5	0.5	0.5	dm^3/kg water
2	V_A	0.735	0.855	0.847	0.855	dm^3/kg soil
3	W_N	0.128	0.082	0.072	0.083	kg w/kg soil
4	W_M	0.219	0.250	0.240	0.249	kg w/kg soil
5	W_{sat}	0.319	0.426	0.417	0.426	kg w/kg soil
6	k_N	410	184	86	71	kg soil/kg w
7	k_M	−37	−20	−19	−19	kg soil/kg w
8	E_{ma}	0.4	1.0	1.6	1.7	Joule/kg soil
9	α_M	75.0	68.6	66.7	68.7	kg soil/kg w
10	σ	0.0001	0.0001	0.0001	0.0001	kg w/kg soil
11	k_{ma^o}	1.7×10^{-10}	8.8×10^{-12}	1.0×10^{-11}	8.5×10^{-12}	dm/s
12	α^o	278	238	194	238	kg soil/kg w
13	E_{mi}	6.8	13.8	21.2	23.7	Joule/kg soil
14	$t_{1/2}$	30	30	30	30	min
15	k_{sat}	9.0×10^{-06}	2.6×10^{-04}	1.6×10^{-04}	2.6×10^{-04}	dm/s

Table 4. Kamel® parameters estimated for the Yolo loam Soil in Davidson et al. (1969) using KamelSoil® given the texture, the bulk density and the soil moisture at saturation.

no.	Parameters	horizon1	horizon2	horizon3	horizon4	Units
1	K_{bs}	0.605	0.535	0.535	0.535	dm^3/kg w
2	V_A	0.65	0.77	0.77	0.77	dm^3/kg soil
3	W_N	0.07	0.08	0.08	0.08	kg w/kg soil
4	W_M	0.21	0.23	0.23	0.23	kg w/kg soil
5	W_{sat}	0.32	0.43	0.42	0.43	kg w/kg soil
6	k_N	212.32	197.38	195.22	197.38	kg soil/kg w
7	k_M	−32.22	−26.99	−27.92	−26.99	kg soil/kg w
8	E_{ma}	0.71	0.7	0.67	0.7	Joule/kg soil
9	α_M	70	48	48	48	kg soil/kg w
10	σ	0.0017	0.0005	0.0003	0.0005	kg w/kg soil
11	k_{ma^o}	4.21×10^{-11}	1.16×10^{-11}	1.94×10^{-11}	1.16×10^{-11}	dm/s
12	α^o	501	389	360	389	kg soil/kg w
13	E_{mi}	17.47	18.4	18.78	18.4	Joule/kg soil
14	$t_{1/2}$	30	30	30	30	min
15	k_{sat}	5.75×10^{-05}	2.04×10^{-04}	1.75×10^{-04}	2.04×10^{-04}	dm/s
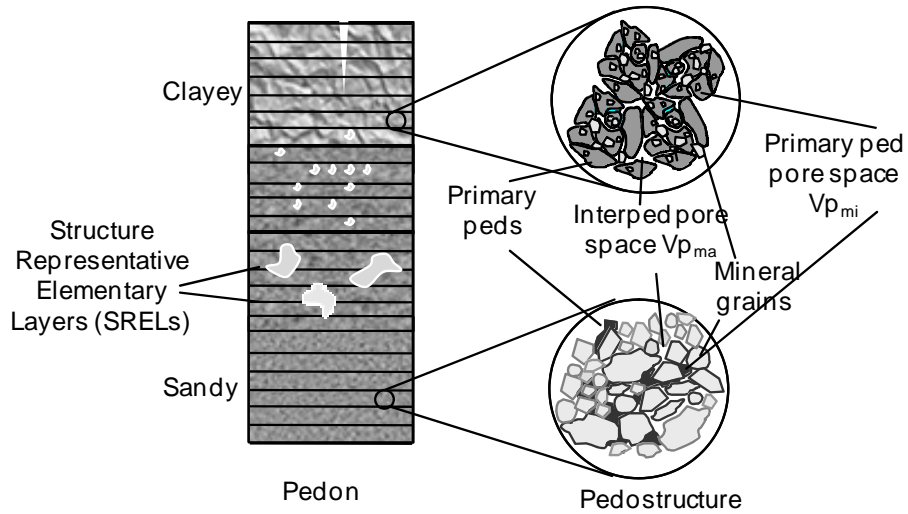
Fig. 1. Soil medium organization.

w_{ip}+max(w_{st})

Primary peds

w_{st}

w_{bs}+max(w_{re})

Primary particles

w_{re}

Spaced

Joined
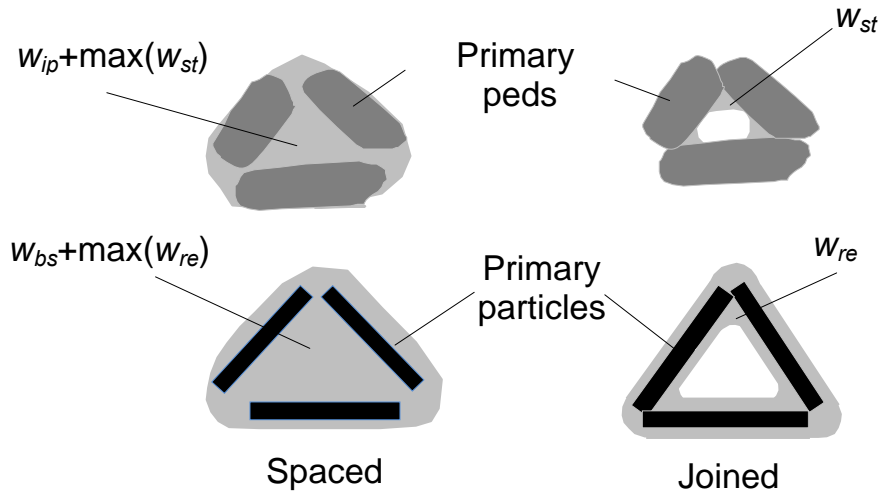
Fig. 2. Schematic definition of the four types of water within the inter and intra primary peds spaces.
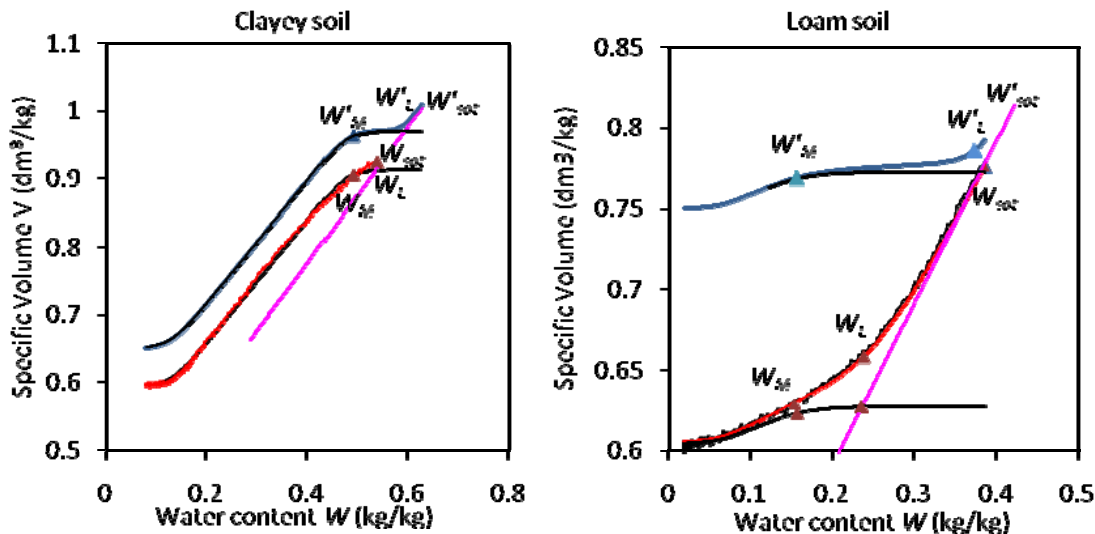
Fig. 3. Various shapes of shrinkage curves: the two shrinkage curves (S_hC) in the same graph differ only by effect of three characteristics: BD (Bulk Density at moist state), W_L and k_L. Curves in black on the graphic on the right represent the shrinkage curve if the interped swelling water, w_{ip}, is not taken into account ($w_{ip}=0$ in Eq. (5) of the S_hC). The curves in blue dots are measured curves (Ferrisol in Martinique and loam soil of Indiana).

Medium variables relationships:

$$d\overline{V} = K_{bs}\,dw_{bs} + K_{ip}\,dw_{ip}$$
$$Vp = Vp_{mi} + Vp_{ma}$$
$$W = W_{ma} + W_{mi}$$
$$W_{mi} = w_{bs} + w_{re}$$
$$W_{ma} = w_{st} + w_{ip}$$
$$\overline{V_{mi}} = Vp_{mi} + 1/\rho_s$$
$$Vp_{mi} = (\max(w_{re}) + w_{bs})/\rho_w$$
$$Vp_{ma} = \overline{V} - \overline{V}_{mi}$$

Pedostructure unit of specific volume $\overline{V}$

S-matrix ($\overline{V_{mi}}$)

air

air

air

air

- Interpedal porosity
- Primary ped medium
- Darcian water transfer
- Micro-macro and micro-micro water exchange

Macropore water ($w_{st}+w_{ip}$)

Micropore swelling water (w_{bs})+ solids

Micropore residual water (w_{re})+ solids
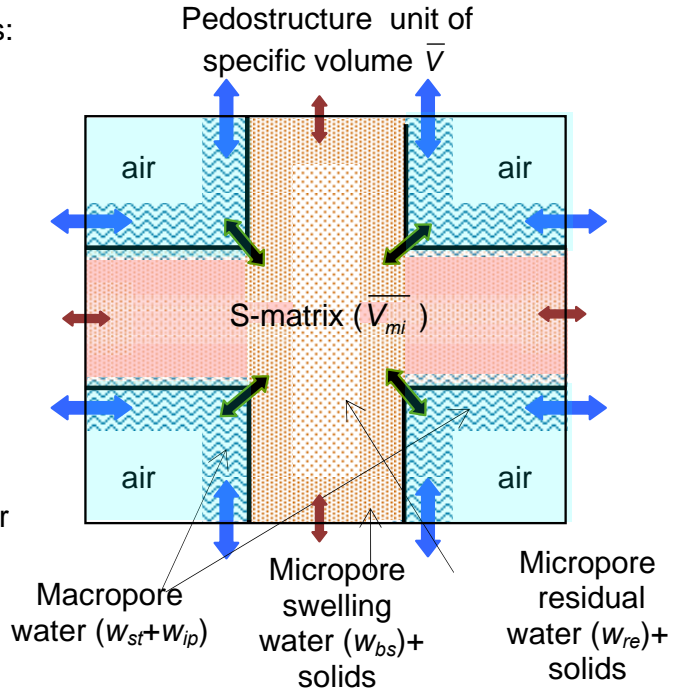
Fig. 4. Schematic representation of the pedostructure, as SREV of the soil medium, and water movements in this medium.

Figure 5
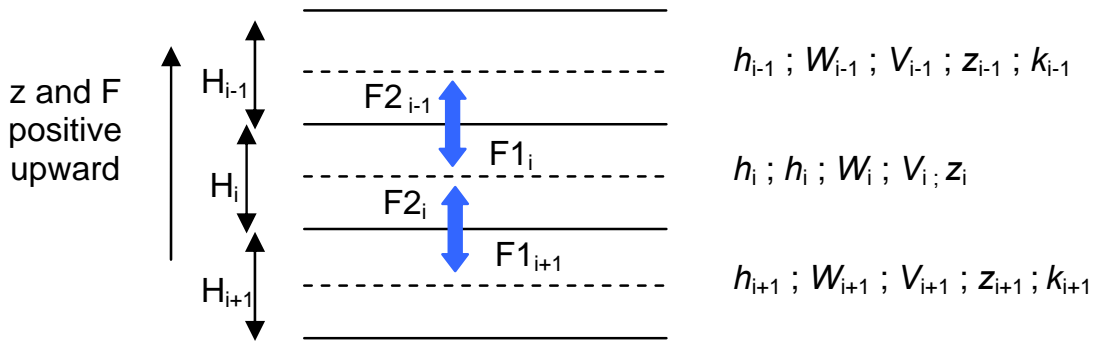
Fig. 5. Representation of three successive soil layers with their associated state variables resulting from the discretization of the soil profile into SRELs. The dashed line represents the middle of the layer. The fluxes through each surface of the layers are such that $F2_{i-1} = F1_i$ and $F2_i = F1_{i+1}$.
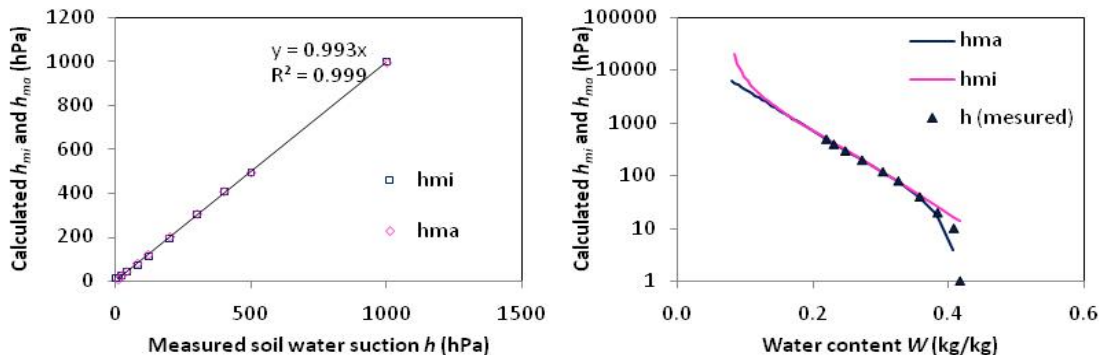
1158

Figure 6

Fig. 6. Example of calculated micro and macro soil water suctions, h_{mi} and h_{ma}, for the Yolo loam soil sample (60 cm) in Davidson et al. (1969): **(a)** fitted on the measured soil moisture characteristic curve $h(W)$ from 0 to 500 hPa; and **(b)** with h_{mi} forced to pass by the estimated point (W_{1500}, h=1500 kPa).
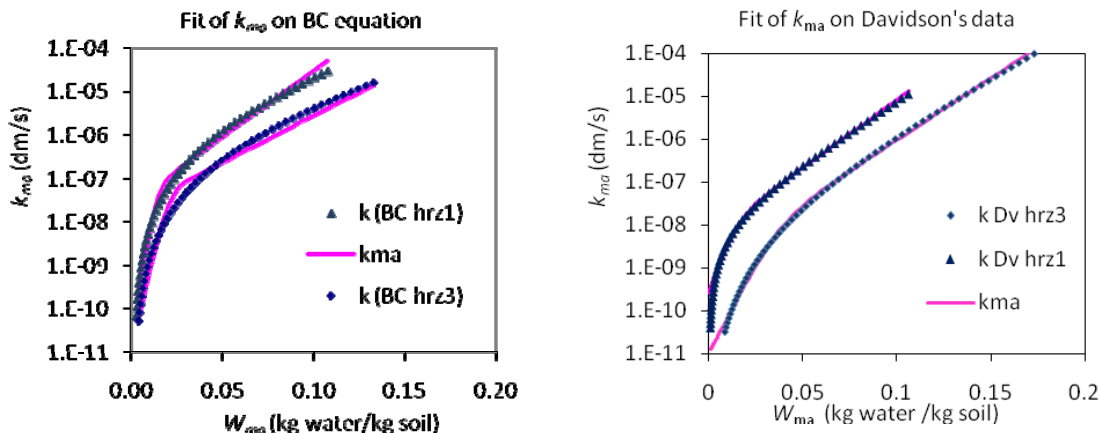
Figure 7

Fig. 7. Hydraulic conductivity parameters obtained by optimizing the fit of the exponential logistic equation of k_{ma} on: **(a)** the estimated Brooks and Corey's equation of the conductivity k for horizons 1 and 3 of the Yolo loam Soil using KamelSoil®; and **(b)** on the measured exponential equation of the conductivity for the same horizons (Davidson et al., 1969).
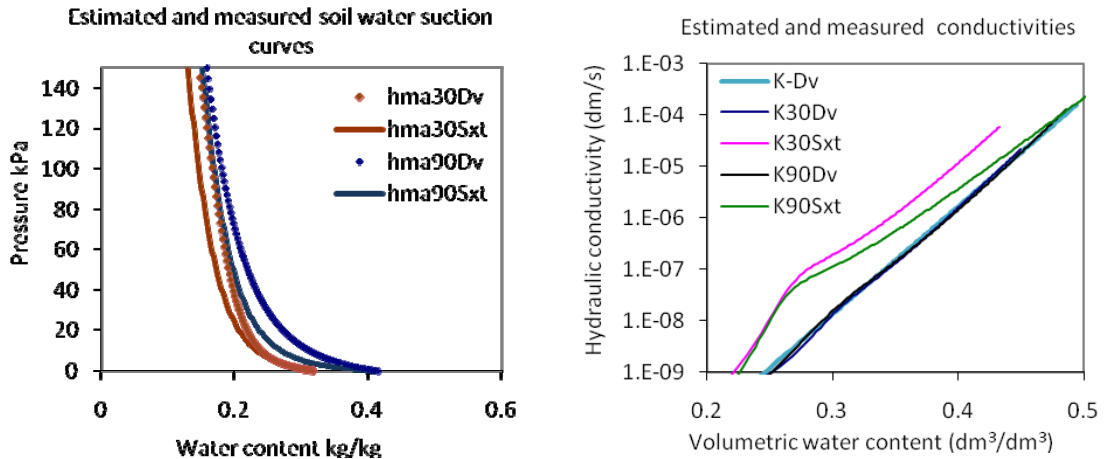
Figure 8

Fig. 8. Soil water suction and hydraulic conductivity curves for 30 cm and 90 cm depth of the Yolo loam Soil. DV refers to as data of Davidson et al. (1969) and Sxt refers to as data estimated according to Saxton and Rawls (2006) using KamelSoil®.
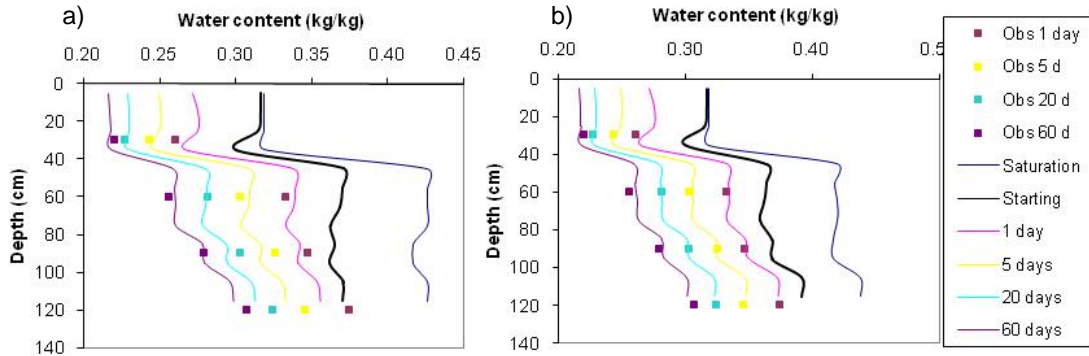
Fig. 9. Simulation of drainage after infiltration up to equilibrium (black line "starting") in the Yolo loam soil profile (Davidson et al., 1969). Squares represent the measured observations and lines represent the simulated moisture profile using the measured soil characteristic parameters given in the article: **(a)** without any change of these parameters and **(b)** with a correction of the parameter W_{sat} for the second and fourth horizon corresponding to the deviation of water content at one day (−0.006 kg/kg and +0.02 kg/kg, respectively).
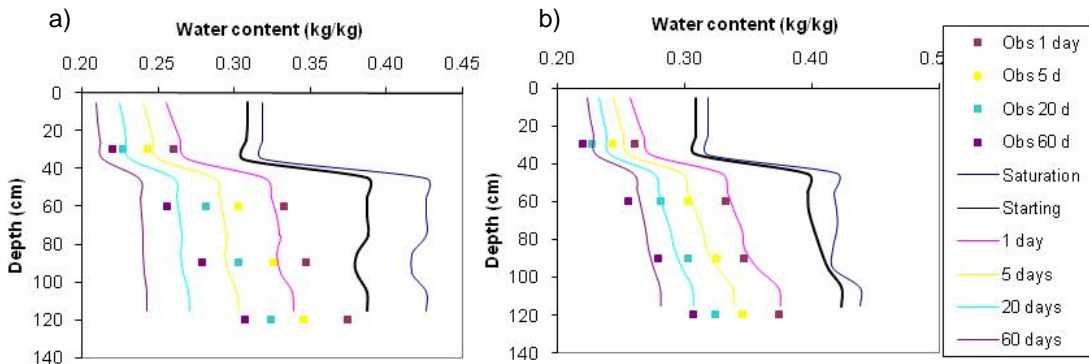
Fig. 10. Simulation of Davidson et al. (1969) field experiment using characteristic parameters estimated by KamelSoil® using pedotransfer functions according to Saxton and Rawls (2006): **(a)** without any change of parameters and **(b)** with a correction of k_{sat} calculated from the deviation of water content at one day (Eq. 36).